



THREE-DIMENSIONAL ELLIPTIC FOURIER METHODS FOR THE PARAMETERIZATION OF HUMAN PINNA SHAPE

Carl Hetherington, Anthony I. Tew, Yufei Tao

Department of Electronics
University of York, Heslington, York YO10 5DD

ABSTRACT

This paper describes an extension to existing work on three-dimensional elliptic Fourier descriptors (see [1]) which enables the efficient parameterization of human pinna shape. The theory and implementation of the new method are discussed and examples of pinna shape parameters given. We describe an application of the method to the estimation of the acoustic pressure response of human pinnae and discuss ongoing work into the parameterization of full head shapes.

1. INTRODUCTION

The elliptic Fourier transform (EFT) is a long-established method for decomposing two-dimensional contours into Fourier components (see, for example, [2]). Its principle is to take a two-dimensional contour in xy and to parameterize it in terms of a third variable t as $x(t)$ and $y(t)$. These components are then subjected to Fourier transforms to give spectra for the contour's x and y components.

Park and Lee [1] have demonstrated a method by which the EFT can be extended into three dimensions. They consider a three-dimensional representation of a human body shape aligned along the z axis and take cross sections for various values of z . The cross-sectional shapes are transformed with a 2D EFT and the resulting spectra are then subjected to a second Fourier transform along z .

2. APPLICATION OF EFT TO PINNA SHAPE

Our research is motivated by the desire to parameterize the shape of the human pinna. While the EFT would seem to be an appropriate method, the approach of Park and Lee [1] is ill-suited to this particular class of shapes. The cross sections taken along any Cartesian axis of a typical pinna mesh, like that in Figure 1, will almost always consist of multiple contours which cause rather significant complexities in the transform process.

We propose a modification to the work of Park and Lee which is better suited to our application. Instead of taking cross-sectional 'slices' for the transform inputs, we start

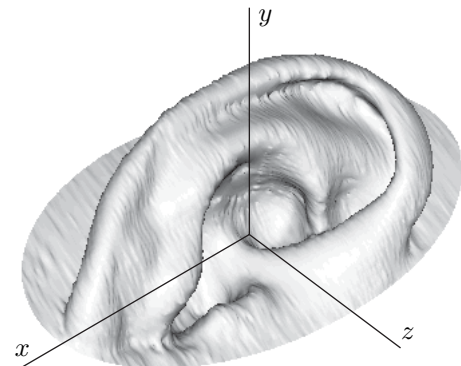


Fig. 1. Example pinna mesh showing alignment with the Cartesian axes

with a slice in the xy plane. An incremental rotation about the y axis then generates each successive slice. This slicing scheme has the advantage of yielding single contours on each slice for a wide range of human pinna shapes.

3. THE MODIFIED EFT METHOD

The first stage in our modified EFT parameterization is alignment. The slicing procedure to follow requires that target pinna meshes are aligned such that the y axis follows the approximate line of the ear canal, as shown in Figure 1. Slice contours can then be obtained using our modified scheme. The xy plane is intersected with the pinna mesh to yield the first contour. This process is then repeated with the plane rotated by a set of S different angles θ around the y axis. We define a rotational step α such that $\alpha = 2\pi/S$. This gives a plane rotation angle $\theta = 0, \alpha, 2\alpha, \dots, 2\pi - \alpha$ and hence a set of S slice contours. Due to the common shape properties of the human pinna, it is postulated that the slices will all contain *single* contours. Exceptions to this rule may exist, but observations suggest that significant problems will be rare. To expedite further processing, each slice is re-orientated to lie in the xy plane by applying appropriate

counter-rotations of $-\theta$ about the y axis.

Due to the nature of the source mesh data, the points making up the slice contours will at this stage be irregularly spaced. They are regularized by means of a simple straight-line interpolation so that each contour has the same number of points, T . The contours can then be described by a pair of functions $f_s^x[t]$ and $f_s^y[t]$ for the x and y components respectively, where s is the slice number that produced the contour, $s = 0, 1, 2, \dots, S-1$ and $t = 0, 1, 2, \dots, T-1$.

The elliptic Fourier transform is most often used for closed contours. Such contours are well suited to the Fourier transform since their x and y components are periodic. In order to force periodicity upon our slice contours, we set t to traverse the contour from one end to the other before returning back to its starting point. In other words, we add the points $t = T-2, T-3, \dots, 2, 1$ to the end of the contour, meaning that it has a new number of points $T' = 2(T-1)$. This has the additional effect of making the slice components into even functions.

The standard approach of Park and Lee [1] is then followed. Let $A_x[s, n]$ and $A_y[s, n]$ be the Fourier coefficients of $f_s^x[t]$ and $f_s^y[t]$ respectively. Since $f_s^x[t]$ and $f_s^y[t]$ are real and even, the spectra $A_x[s, n]$ and $A_y[s, n]$ will be real and Hermitian. We perform the transform operations separately on both f_s^x and f_s^y ; only the working for f_s^x is shown here. The first stage is to calculate $A_x[s, n]$ using the standard discrete Fourier transform expression

$$A_x[s, n] = \sum_{t=0}^{T'-1} f_s^x[t] e^{-jnt/T'} \quad (1)$$

for $n = 0, 1, 2, \dots, T'-1$. We then take a second transform of $A_x[s, n]$ with respect to s . Let $B_x[m, n]$ represent the Fourier transforms of $A_x[s, n]$ so that

$$B_x[m, n] = \sum_{s=0}^{S-1} A_x[s, n] e^{-jms/S} \quad (2)$$

for $m = 0, 1, 2, \dots, S-1$.

When performed for both the x and y components, this method results in a Fourier coefficient set of $B_x[m, n]$ and $B_y[m, n]$. A plot of the low-order values of $\Re\{B_x[m, n]\}$ is shown in Figure 2 as an example; plots of the other parameters show a similar energy distribution but are omitted to save space. The example plot shows the parameter region which contains all the energy.

It is interesting to note some properties of the coefficients which occur because of the way in which slices are taken. Given a set of S slices, spanning slice plane rotation angles from 0 to 2π , the contour on slice $S/2$ will be the same shape as that on slice 0 but in the opposite direction. Thus it is useful to consider the slice collection as two

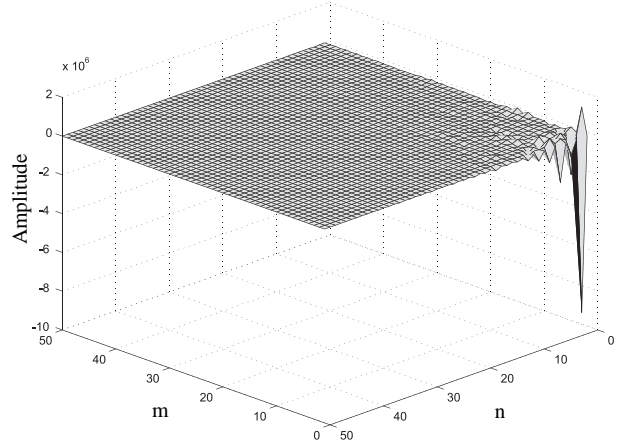


Fig. 2. Plot of the low-order values of $\Re\{B_x[m, n]\}$

subsets. Let

$$\mathbf{v} = \{0, 1, 2, \dots, (S/2) - 1\} \quad (3)$$

$$\mathbf{w} = \{(S/2), (S/2) + 1, (S/2) + 2, \dots, S-1\} \quad (4)$$

There will be close relationships between slices \mathbf{v} and \mathbf{w} as follows:

$$f_{\mathbf{v}}^x[t] = -f_{\mathbf{w}}^x[-t] \quad (5)$$

$$f_{\mathbf{v}}^y[t] = f_{\mathbf{w}}^y[-t] \quad (6)$$

In other words, the x component of the second-half slice contours will be time-reversed and inverted and the y component merely inverted. The properties of the Fourier transform are such that the spectra of x and y will be constrained as follows

$$A_x[\mathbf{v}, n] = -A_x^*[\mathbf{w}, n] \quad (7)$$

$$A_y[\mathbf{v}, n] = -A_y^*[\mathbf{w}, n] \quad (8)$$

This in turn means that the inputs to the second stage transforms will have special properties:

- x inputs — half-wave symmetric
- y inputs — double-periodic (the second half of the input set will be the same as the first)

This means that the second transform spectra B_x will have zero odd harmonics and B_y will have zero even harmonics. These constraints further reduce the number of coefficients that are required to fully describe a parameterized pinna mesh.

3.1. Reconstruction

An important requirement for our intended application is an algorithm to provide good-quality reconstructions of pinna parameters. The reconstruction of the original contours requires only a set of inverse Fourier transforms, and we have developed a simple algorithm to generate full meshes from these contours.

The algorithm consists of a method for joining two adjacent slice contours together. This method is then repeated for each adjacent pair of slices in the set. Given the first pair of contours f_0 and f_1 , we select a ‘point skip’ value p depending on the density of the mesh that is required. We then run through the points of f_0 joining each point $t = 0, p, 2p, \dots$ to the nearest point on f_1 . Adjacent lines are then built into quadrilaterals which make up the mesh. The points to which lines are joined on f_1 are noted in a list J . This process is illustrated in Figure 3.

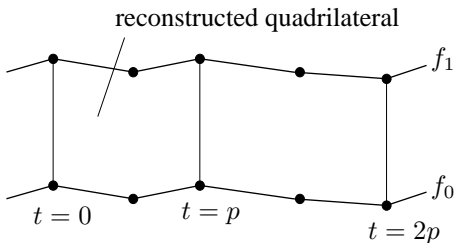


Fig. 3. Joining two slices together during reconstruction

The algorithm then moves on to joining $f_1(t)$ to $f_2(t)$. The first step is to check that points in the list J are reasonably evenly spaced. After several contour pairs have been joined there is a danger of the situation illustrated in Figure 4 whereby gaps open up between the points in the list J . The algorithm checks for these gaps appearing, and any distance between adjacent points in J that exceeds $2p$ is filled in with a new point between the two. Once J has been regularized in this way, the points of $f_1(t)$ in J are joined to the nearest points on $f_2(t)$. The algorithm continues as such until all contours have been joined together. An example of a mesh reconstructed using this algorithm is given in Figure 5.

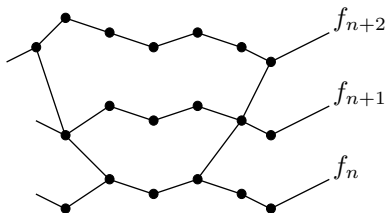


Fig. 4. Illustration of the problem of drift during reconstruction

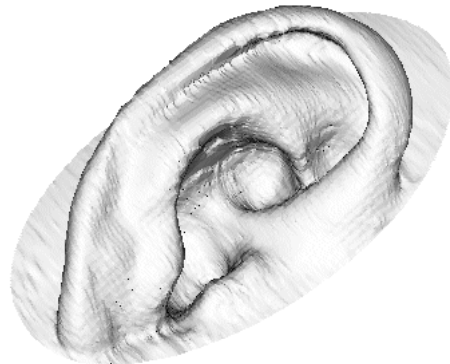


Fig. 5. Example of a reconstructed pinna mesh

4. DISCUSSION

The example parameter set shown in Figure 2 demonstrates that the method expresses the sample pinna shape in a compact form. In particular, the the second Fourier transform is effective due to the similarity between adjacent slices of the pinna shape. This similarity exists because of the relatively slow variation in the shape of the pinna as a function of θ and is exploited by the method.

It is thought that a significant proportion of the ‘energy’ contained in the parameter set is due to the pinna’s slices being open contours. Because of this, the method incorporates the step of forcing the contours to be closed by traversing the contour from beginning to end and back to the beginning, as described in Section 3. While this improves the situation, it still causes a discontinuity in gradient at the end of the slice which will cause the spectrum to contain more energy than it otherwise might.

This problem is largely obviated by developments to the method that we are currently undertaking. Instead of parameterizing a single pinna shape, we are investigating the extension of the same parameterization system to handle an entire human head shape. In this situation, the slice contours obtained from the source mesh are continuous, improving the efficiency of the parameterization. The nature of the human head shape also introduces significant possible savings due to its near symmetry about the the median plane.

Further ongoing work is dedicated to investigating the amount of data compression that the parameterization can offer. Truncating the Fourier transforms at either stage of the process will reduce the number of parameters at the cost of shape detail. The resulting shape errors can be quantified in a variety of ways. We intend to investigate error metrics based on geometric shape difference and also pressure response difference when shapes produced from truncated parameters are used in acoustic models.



5. APPLICATIONS

The intended application of our method is the efficient estimation of acoustic pressure responses. The shape of the pinna strongly influences a person's head-related transfer functions (HRTFs). These HRTFs are the basis of many current spatialised sound systems (see, for example [3]), but are difficult to measure and time-consuming to model numerically. Tao *et. al* [4] have demonstrated a way of making good estimates of human head pressure responses in a very short time. Their method is based on the parameterization of human head shape using surface-spherical harmonics (SSH).

The problem with SSH for the estimation of full HRTFs is that they cannot easily represent the complex shape of the pinna. It is our intention to develop a modified system which replaces SSH with the EFT parameters described in this paper. It is hoped that this will allow the efficient estimation of both pinna and full head pressure response, and in turn full HRTFs.

6. CONCLUSION

In this paper we propose a new type of three-dimensional elliptic Fourier transform. This transform is particularly well-suited to the shape of human pinnae, and allows an efficient parameterization of pinna shape. The transform is distinguished from previous EFT methods by the modified slicing scheme, which eliminates the problems of multiple slice contours and takes advantage of the smooth and slowly-changing nature of the pinna's shape.

Applications include the estimation of acoustic pressures for the human pinna based on shape data. We discuss extensions to the method to include head shape for the purpose of estimating HRTFs.

7. ACKNOWLEDGEMENTS

This work was performed as part of an EPSRC research studentship. The authors would like to thank the developers and users of VTK and 3D Slicer for all their help. We would also like to thank Mr. Yves Martel of Tomovision for his assistance in reading CT scan data. We are indebted to the staff of York District Hospital for their assistance in obtaining CT scans.

8. REFERENCES

- [1] K. S. Park and N. S. Lee, "A three-dimensional Fourier descriptor for human body representation/reconstruction from serial cross sections," *Computers and Biomedical Research*, vol. 20, pp. 125–140, 1987.
- [2] F. P. Kuhl and C. R. Giardina, "Elliptic Fourier features of a closed contour," *Computer Graphics and Image Processing*, vol. 18, pp. 236–258, 1982.
- [3] D. Hammershøi and H. Møller, "Methods for binaural recording and reproduction," *Acustica*, vol. 88, no. 3, pp. 303–311, 2002.
- [4] Y. Tao, A. I. Tew, and S. J. Porter, "The differential pressure synthesis method for estimating acoustic pressures on human heads," in *Proc. AES 112th convention, Munich*, 2002.